Inorg. Chem. **2005**, *44*, 5981–5983

Isolated Magnetic Clusters of Co(II) and Ni(II) within 3-Dimensional Organic Frameworks of 6-Mercaptonicotinic Acid: Unique Structural Topologies Based on Selectivity for Hard and Soft Coordination Environments

Simon M. Humphrey,[†] Richard A. Mole,[†] Mary McPartlin,[‡] Eric J. L. McInnes,[§] and Paul T. Wood*[,†]

University Chemical Laboratory, University of Cambridge, Lensfield Road, Cambridge CB2 1EW, U.K., Department of Health and Biological Sciences, London Metropolitan University, London N7 8DB, U.K., and Department of Chemistry, University of Manchester, Oxford Road, Manchester MN13 9PL, U.K.

Received May 13, 2005

Hydrothermal reaction of the mixed thiolate–carboxylate–aromatic amine ligand, 6-mercaptonicotinic acid (6-mnaH$_2$) with Co(II) and Ni(II) leads to two network coordination solids [M$_9$(6-mna)$_8$(μ_3-O)$_2$(OH$_3$)$_2$(OH$_2$)$_6$] (M = Co, Ni), **1**, and [M$_2$Ni$_{12}$(6-mna)$_{12}$(μ_3-OH)$_2$(OH$_2$)$_6$]·8H$_2$O (M = K, Rb, Cs), **2**. These compounds are unusual for two reasons: they are thiolate-bridged networks and they are three-dimensional lattices which contain isolated metal clusters and chains. The magnetic behavior of these compounds has been studied, showing that **2** contains ferromagnetically coupled Ni$_6$ wheels.

The formation of new magnetic materials incorporating organothiolate ligand frameworks is an intriguing proposition in materials synthesis. While very few such compounds have previously been reported[1] in comparison to the many oxygen-bridged species,[2] thiolate-*S* is desirable as a single-atom bridge between adjacent 3d-metal centers. Better matching of orbital energies leads to greater concentration of spin density onto the bridging atom and therefore stronger magnetic superexchange.[3] This is beneficial both in single-molecule magnets and in model compounds for the study of low-dimensional magnetism. Moreover, from a synthetic standpoint, new structural types may also be observed due to the provision of both linear and bent coordination geometries via thiolate-*S*.[1]

Our studies into the hydrothermal synthesis of new materials using mixed thiolato-carboxylate ligands such as 6-mercaptonicotinic acid (6-mnaH$_2$), (NC$_5$H$_3$(CO$_2$H)(SH)-3,6), has led to the identification of three intriguing new coordination polymers. These materials are defined not only by the presence of high-symmetry magnetic clusters isolated within extended lattices but also by curious selectivity of Co(II)/Ni(II) ions for both hard-only (carboxylate- and hydroxide/oxide-*O*) and soft-only (pyridine-*N*, thiolate-*S*) donor sets. Reaction of NiCl$_2$ and 6-mnaH$_2$ with excess CsOH in water at 210 °C was found to produce, upon slow cooling, a mixture of two crystalline phases that were subsequently prepared in pure form via minor alterations to the reaction conditions. Single-crystal X-ray diffraction studies[4,5] identified clusters of dark red square plates as [Ni$_9$(6-mna)$_8$(μ_3-O)$_2$(OH$_3$)$_2$(OH$_2$)$_6$], **1a**, and tiny green hexagonal rods as [Cs$_2$Ni$_{12}$(6-mna)$_{12}$(μ_3-OH)$_2$(OH$_2$)$_6$]·8H$_2$O, **2**. It was found upon further experimentation with other alkali metal hydroxides (Li, Na, K, Rb) and 3d-metal(II) salts that an analogue of **1a** could be formed using CoCl$_2$, **1b**.[6] **2** may also be made in very low yields (<5%) with K and Rb but not with Li or Na. We attribute this synthetic control to the

* To whom correspondence should be addressed. E-mail: ptw22@cam.ac.uk.
[†] University of Cambridge.
[‡] London Metropolitan University.
[§] University of Manchester.

(1) (a) Humphrey, S. M.; Mole R. A.; Rawson, J. M.; Wood, P. T. *Dalton Trans.* **2004**, 1670−1678. (b) Cave, D.; Gascon J−M.; Bond, A. D.; Teat, S. J.; Wood P. T. *Chem. Commun.* **2002**, 1050−1051. (c) Han, L.; Hong M.; Wang, R.; Wu, B.; Xu, Y.; Lou, B.; Lin, Z.; *Chem. Commun.* **2004**, 2578−2579.
(2) See, for example: (a) Policar, C.; Lambert, F.; Cesario, M.; Morgenstern-Badarau, I. *Chem. Eur. J.* **1999**, 2201−2207. (b) Kim, J.; Chen, B.; Reineke, T. M.; Li, H.; Eddaoudi, M.; Moler, D. B.; O'Keeffe, M.; Yaghi, O. M. *J. Am. Chem. Soc.* **2001**, *123*, 8239−8247. (c) Rao, C. N. R.; Natarajan, S.; Vaidhyanathan, R. *Angew. Chem., Int. Ed.* **2004**, *43*, 1466−1496.
(3) Kahn, O. *Molecular Magnetism*; Wiley-VCH: New York, 1993.
(4) Crystal data for **1a**, C$_{48}$H$_{42}$N$_8$Ni$_9$O$_{26}$S$_8$: M = 1931.77, tetragonal, space group $I4_1/acd$, $a = b$ = 13.9938(2) Å, c = 62.1034(9) Å, V = 12161.5(3) Å^3, Z = 8, T = 180(2) K. Refinement of 257 parameters on 2673 independent reflections out of 22 565 total measured reflections (R_{int} = 0.0873) led to R1 = 0.0402, wR2 = 0.0988, and S = 1.043. Crystal data for **2**, C$_{72}$H$_{66}$Cs$_2$N$_{12}$Ni$_{12}$O$_{40}$S$_{12}$: M = 3094.41, trigonal, space group $P\bar{3}$, $a = b$ = 19.0136(3) Å, c = 8.5131(2) Å, V = 2665.30(9) Å^3, Z = 1, T = 180(2) K. Refinement of 237 parameters on 3107 independent reflections from 9498 total measured reflections (R_{int} = 0.0399) gave R1 = 0.0299, wR2 = 0.0720, and S = 1.042.
(5) Sheldrick, G. M. *SHELXTL*, Version 6.10; Bruker AXS, Inc.: Madison, WI, 2001.
(6) The structure of **1b** was confirmed by comparing its X-ray powder diffraction pattern with that of **1a**, in addition to obtaining satisfactory characterizing data.

10.1021/ic050768q CCC: $30.25
Published on Web 07/26/2005

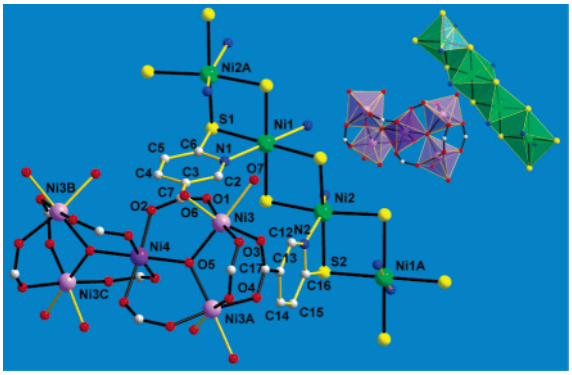

Figure 1. Extended asymmetric unit of **1a** with magnetic exchange pathways drawn in black. Inset: polyhedral representation of isolated chain and twisted bowtie topologies with organic fragments omitted.

larger ionic radius of Cs being more closely matched to the size of cavities in the lattice of **2** in which the metal ions are located.

A view of the extended asymmetric unit of **1a** (Figure 1), which crystallizes in the tetragonal space group $I4_1/acd$ ($Z = 8$), clearly shows two distinct magnetic topologies: octahedral Ni(II) centers (Ni1 and Ni2) are bis-chelated by 6-mna ligands, via four-membered (−CN−Ni−S−) rings with pyridine-*N* arranged trans and equatorial thiolate-*S* that bridge adjacent metal centers with angles of 91.31(3)° and 91.12(3)° (at S1 and S2, respectively). An undulating chain of edge-sharing Ni(II) octahedra is formed (Figure 1 inset) of squares of (−Ni1−S1−Ni2−S2−) repeat units, with adjacent pairs of chelating ligands on alternating faces of the chain. Isolated Ni_5 clusters are comprised of *syn,syn-OCO*-carboxylate bridges (a) between symmetry equivalents of Ni3 and (b) between Ni3 and unique octahedral Ni4 which is present on the 4-fold site. The slightly distorted octahedral environment of Ni3 is comprised of two *cis*-OH_2/OH_3^+, three *meridinal*-carboxylates bridging to Ni4, and an equivalent Ni3 via a trigonal-planar μ_3-oxide bridge (O5). Charge balance requires that the OH_2/OH_3^+ ratio is 3:1. X-ray data provide an average Ni−O bond distance of 2.055(4) Å. In comparison to literature values, this is marginally longer than expected for a $Ni^{2+}-O^{2-}$ covalent interaction. The presence of O^{2-} and H_3O^+ on the same cluster is unusual; however, in this case, it is favorable as it facilitates very close H-bond-mediated intercluster contacts. Water ligands on adjacent clusters are separated by between 2.887(2) and 2.937(2) Å, which is only reasonable when H-bonding is present. In addition, the H-bonds have bridging angles close to 180°. The overall topology of the O-bridged cluster is a twisted bowtie of vertex-sharing octahedra where the angle between adjacent triangles is found to be 34.8°. In addition, subsequent EPR studies on **1a** confirmed that no neutral thiolate radicals or Ni(III) are present,[7] adding weight to our interpretation of the crystal structure determination. The extended lattice of **1a** (Figure 2) takes the form of layers of chains and clusters separated by ligand fragments. Alternate layers of chains are aligned orthogonally, lying parallel to

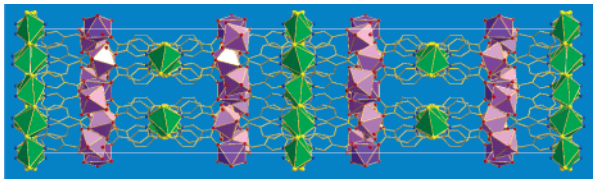

Figure 2. Unit cell of **1a** in the *bc* plane showing layers of chains and clusters with alternate layers of chains running parallel to *a* and *b*.

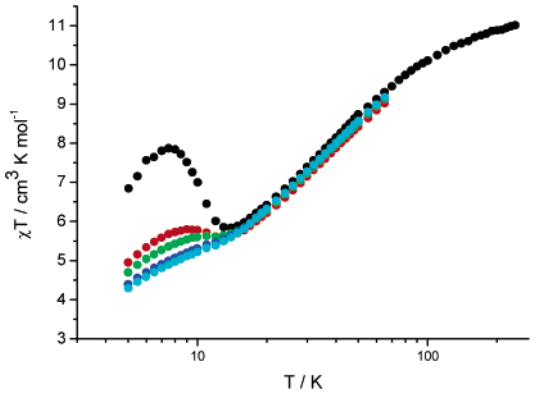

Figure 3. Graph of χT vs T for compound **1a** in various applied fields. Black, 100 G; red, 500 G; green, 1000 G; blue, 5000 G; cyan, 10 000 G.

the crystallographic *a* and *b* axes, while clusters are arranged in sheets in the *ab* plane, in a herringbone array. The magnetic behavior of **1a** shows a transition at 14 K (seen in Figure 3) to a phase with a small spontaneous moment, but isothermal magnetization measurements show a very small coercive field. The Curie constant $C = 11.8$ cm^3 mol^{-1} K is reasonable for nine Ni(II) ions, and the Weiss constant of −17.5 K indicates that the dominant exchange interaction is antiferromagnetic. The field-dependence of χT vs T shows that the source of the spontaneous moment is probably spin-canting, as the maximum at low temperatures *decreases* with *increasing* applied field. The magnetic behavior of **1b** is similar, with a phase transition at approximately 30 K but a very small coercive field. The Weiss constant (−53 K) is consistent with a higher T_C, and the Curie constant (27.8 cm^3 mol^{-1} K) is reasonable for nine Co(II) ions. In both **1a** and **1b**, there will be areas of short-range order at temperatures above the magnetic phase transitions. Superexchange within the chains and bowtie clusters will be stronger than dipolar coupling between these features; therefore, the short-range order will be contained within these moieties.

In contrast to the mixed chain and cluster topology in **1a**, the very unusual alkali metal-containing phase **2** that crystallizes into the trigonal space group $P\bar{3}$ ($Z = 1$), is comprised of a lattice of two different types of magnetic clusters (Figure 4). There is again a stark preference for Ni(II) to attain N,S- or O-only donor sets, which are similar in connectivity to that observed in **1a**. *N,S*-Ni_6 rings are formed by bis-thiolate bridging between adjacent octahedral Ni(II) centers with cis-oriented pyridine-*N* of chelating 6-mna situated on the periphery of the ring. Alternate squares of (−Ni1−S1−Ni1A−S1A−) are oriented almost orthogonally (89.8°, considering mean planes of the rings), such that every other thiolate-*S* atom on each face of the ring form Cs1−S1 contacts with an average distance of 3.487(1) Å (Figure 3,

(7) Ray, K.; Weyhermuller, T.; Goossens, A.; Crajé, M. W. J.; Wieghardt, K. *Inorg. Chem.* **2003**, *42*, 4082−4087.

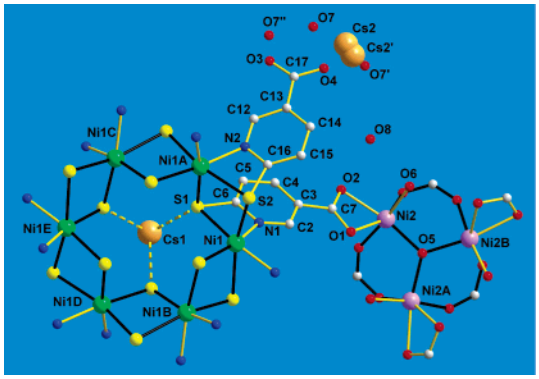

Figure 4. Extended asymmetric unit of **2**: *N*,*S*-Ni_6 rings and *O*-Ni_3 triangle clusters.

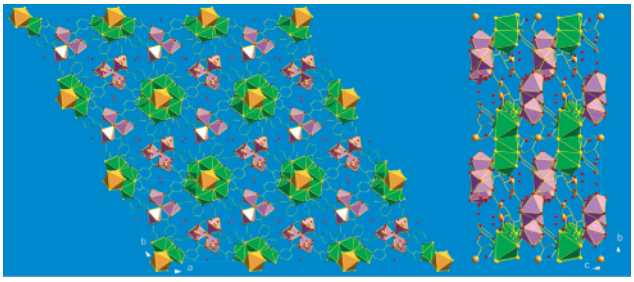

Figure 5. (a) (left). The *ab* plane of **2** displaying hexagonal network of clusters (octahedra of Cs(I) also drawn) and lattice H_2O positions within small cavities. (b) (right). Section parallel to the unique axis showing diagonal alignment of clusters and position of Cs(I) cations.

dashed lines). Cs1 ions are located at [0,0,0] and sit directly between adjacent Ni_6 rings, forming an octahedral coordination environment. Ni_3O clusters of highly distorted Ni(II) octahedra are formed on the basis of two types of carboxylate coordination: chelation of Ni2 equivalents by 6-mna with a very small bite angle of 61.3(2) ° on one face of the cluster is accompanied by syn,syn-bridging on the other, forming a bowl-shaped $(-Ni2-O3-C17-O4-)_3$ ring. Ni2 centers are also monohydrated and the coordination environments completed by μ_3-OH (O5), situated at the center of the cluster, having conventional pseudo-tetrahedral geometry. Cs2 ions are equally disordered over small cavities within the structure, each having $^1/_6$ site occupancy, thus giving a single Cs2 per unit cell; the remaining $^5/_6$ cavities are occupied by H_2O of crystallization (O7). Further H_2O of crystallization (O8) are also located within the extended structure of **2**, as seen in a view of the unique plane of **2** (Figure 5a). This solution for **2** shows excellent agreement with microanalysis data (see Supporting Information). The *ab*-plane has a honeycomb lattice of well-isolated Ni_6 and Ni_3 clusters. When viewed in the *ac* and *bc* planes (Figure 5b), it is evident that Ni_6 rings are stacked in rows with Cs(I) ions interspersed while Ni_3 clusters are stacked in a 1,2-type repeating pattern. Clusters are concomitantly arranged in diagonal rows, passing approximately along the *ac* and *bc* bisectors. The magnetic susceptibility of **2** has been simulated using the program MAGPACK[8] using a model consisting of one Ni(II) hexagon and two Ni(II) triangles (Figure 6). This gives $J = +9$ K for the intrahexagon

(8) Borras-Almenar, J. J.; Clemente-Juan, J. M.; Coronado, E.; Tsukerblat, B. S. *J. Comput. Chem.* **2001**, *22*, 985−991.

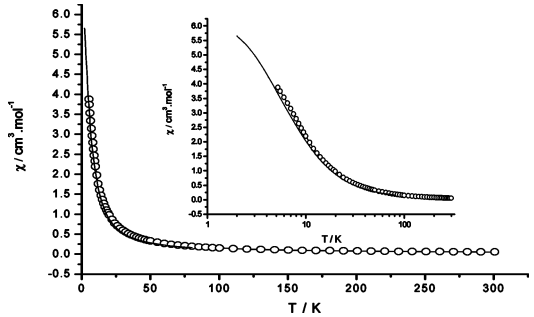

Figure 6. The temperature dependence of the magnetic susceptibility of **2** (for 12 Ni(II) ions) in a field of 100 G and the fit of these data for the MAGPACK model. The inset has a logarithmic *x* axis to emphasize the low-temperature data.

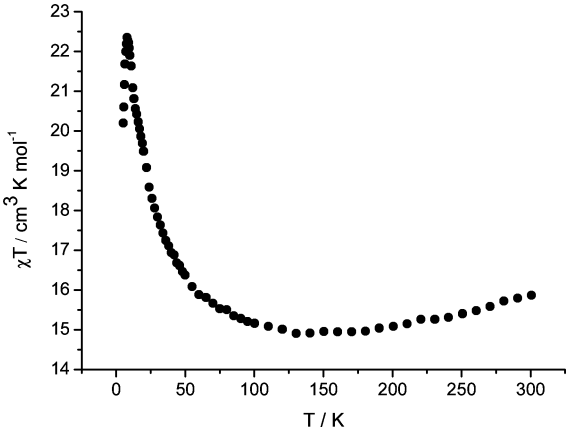

Figure 7. Plot of χT vs T for **2** in a measuring field of 100 G.

coupling and $J = -4.3$ K for the intratriangle interaction. Ferromagnetic intrahexagon and antiferromagnetic intratringle couplings are as expected by consideration of the Goodenough−Kanamori rules[3] as the Ni−S−Ni angles are 89.14(4)° and the Ni−O−Ni angles are 115.59(10)°. The presence of both ferromagnetic and antiferromagnetic coupling results in a minimum in the χT vs T measurement (Figure 7). Despite the stronger exchange expected from thiolate bridges, the intrahexagon coupling is relatively weak due to competition between ferromagnetic and antiferromagnetic components. The Ni_6 clusters embedded within this network have an $S = 6$ ground state and are therefore similar to the purely molecular Ni_{12} and Ni_{24} ferromagnetically coupled clusters of Winpenny and co-workers.[9] Measurements are underway to determine if **2** acts as a single-molecule magnet.

Acknowledgment. We would like to thank Dr. John E. Davies (Cambridge) for assistance in X-ray data collection for **1a** and **2** and the EPSRC (S.M.H., R.A.M.) for funding.

Supporting Information Available: Full experimental methods for **1a**, **1b**, and **2**, including characterizing data; crystallographic data (CIF) for **1a** and **2**; SQUID magnetic data for **1a**, **1b**, and **2**. This material is available free of charge via the Internet at http://pubs.acs.org.

IC050768Q

(9) (a) Dearden, A. L.; Parsons, S.; Winpenny, R. E. P. *Angew. Chem., Int. Ed.* **2001**, *40*, 151−154. (b) Andres, H.; Basler, R.; Blake, A. J.; Cadiou, C.; Chaboussant, G.; Grant, C. M.; Gudel, H. U.; Murrie, M.; Parsons, S.; Paulsen, C.; Semadini, F.; Villar, V.; Wernsdorfer, W.; Winpenny, R. E. P. *Chem. Eur. J.* **2002**, *8*, 4867−4876.